Chaos, Solitons and Fractals 180 (2024) 114504

Contents lists available at ScienceDirect

Chaos, Solitons and Fractals

journal homepage: www.elsevier.com/locate/chaos

First integrals can explain coexistence of attractors, multistability, and loss of ideality in circuits with memristors

Giacomo Innocenti [a,*], Alberto Tesi [a], Mauro Di Marco [b], Mauro Forti [b]

[a] Department of Information Engineering, University of Florence, via di Santa Marta 3, Firenze, 50139, FI, Italy
[b] Department of Information Engineering and Mathematics, University of Siena, Via Roma 56, Siena, 53100, SI, Italy

ARTICLE INFO

Keywords:
Memristor
First integral of the motion
Coexistence of attractors
Multistability
Loss of ideality

ABSTRACT

In this paper a systematic procedure to compute the first integrals of the dynamics of a circuit with an ideal memristor is presented. In this perspective, the state space results in a layered structure of manifolds generated by first integrals, which are associated, via the choice of the initial conditions, to different exhibited behaviors. This feature turns out to be a powerful investigation tool, and it can be used to disclose the coexistence of attractors and the so called "extreme multistability," which are typical of the circuits with ideal memristors. The first integrals can also be exploited to study the energetic behavior of both the circuit and of the memristor itself. How to extend these results to the other ideal memelements and to more complex circuit configurations is shortly mentioned. Moreover, a class of ideal memristive devices capable of inducing the same first integrals layered in the state space is introduced. Finally, a mechanism for the loss of the ideality is conceived in terms of spoiling the first integrals structure, which makes it possible to develop a non-ideal memristive model. Notably, this latter can be interpreted as an ideal memristive device subject to a dynamic nonlinear feedback, thus highlighting that the non-ideal model is still affected by the first integrals influence, and justifying the importance of studying the ideal devices in order to understand the non-ideal ones.

1. Introduction

In the last decade, the interest in the ideal element, theorized in 1971 by Prof. Chua in his pioneering paper [1] and called "memristor", has been stimulated by the discovery of memristive effects in solid-state nanoscale electronic devices with ionic transport subjected to an external bias voltage [2]. Ideal memristors, indeed, are blessed with many properties, which make them suitable candidates for the hardware implementation of a new generation of brain-inspired analog computing machines conceived in the neuromorphic computing paradigm [3–7]. Under this motivation, a vast scientific literature of papers focused on circuits with memristors has been produced, but the community is still debating on very important issues. Indeed, the actual relationship between the ideal memristor and the models describing the memristive effects found in the real devices has not been completely disclosed yet. In fact, it is not even clear in what sense the ideal memristor dynamics can actually be approximated by real memristive devices, which count several different models depending on the physical effect the implementation is based on [5,8–12]. The nature of the nonlinear characteristic function of the memristor is another critical issue, since it also defines the energetic behavior of the element, and many authors argue about the active/passive nature of real implementations and their capability of being at least locally active [13,14]. Despite the debate on the connection between ideal and real memristors is still lively, many papers have been focused on the first one, even though its study is made difficult by the nonlinear nature of the element. Specific investigation techniques have been developed to systematically address this study [15–19], while an important branch of the scientific literature focuses on studying circuits with ideal memristors mainly resorting to numerical techniques and simulations [20,21]. These papers have highlighted the incredible richness of behaviors, that a single circuit with ideal memristors is able to exhibit. Some authors have even coined the term "extreme multistability" to refer to the capability of memristive devices to generate a huge number of coexisting attractors in their state space representation [22,23].

In this paper we will show that, when an ideal memristor is connected to a circuit belonging to a broad class of devices, it induces the existence of a first integral of the motion. Moreover, this special structure corresponds to a reduced order dynamics, which describes the system behavior under the effect of a tuning parameter, which in reality depends on the initial conditions of the circuit. Notably,

* Corresponding author.
E-mail addresses: giacomo.innocenti@unifi.it (G. Innocenti), alberto.tesi@unifi.it (A. Tesi), dimarco@diism.unisi.it (M. Di Marco), forti@diism.unisi.it (M. Forti).

https://doi.org/10.1016/j.chaos.2024.114504
Received 21 November 2023; Received in revised form 18 January 2024; Accepted 19 January 2024
Available online 1 February 2024

this scheme is defined by a nonlinear non-homogeneous differential equation, that can also be seen as a forced feedback system. Reasoning on this premise, in Section 2 it will be illustrated how the first integral can be spotted in a simple circuit with an ideal charge-controlled memristor. The circuit will be investigated highlighting a multistabile dynamics, that can be directly related to the features of the same first integral. In Section 3 it will be shown that the existence of the first integral is a common property for circuits with ideal memristors, and a general procedure for their analytic computation will be presented. In particular, in Section 3.3 the first integrals will be exploited to give a dynamical interpretation of the richness of behaviors exhibited by circuits with memristors, thus providing a structural explanation of their extreme multistability. Section 4 will be devoted to the energetic characterization of circuits with ideal memristors in order to disclose that there is no link between the first integral of the motion and the energy storage. Motivated by the previous results, a new class of "ideal" memdevices able to induce first integrals as well as the original ideal memristor will be introduced in Section 5, and it will be exploited in Section 6 to elaborate on the concept of "loss of ideality," just meant here as the loss of the first integrals structure. Notably, such a loss of ideality does not completely erase the first integrals imprint from the circuit behavior, motivating the proposed non-ideal memristive models as suitable candidates for describing real devices, which then could be investigated applying to their ideal counterpart the proposed tools based on the first integrals.

2. Background and motivation

In the recent literature, many circuits with memristive devices have been introduced for the richness of their dynamics, and especially for their capability of showing complex behaviors in a multistability scenario. This latter property is very desirable in many contexts, but it plays a critical role in the analog computing framework, which is attracting increasing interest thanks to many innovative neuromorphic computing paradigms [3–7]. Such an opportunity has fired up the study of circuits featuring memelements, bringing forth promising results related to their ability of exhibiting multiple different stationary dynamics (e.g., constant and periodic solutions) under the same configuration [24–26]. Indeed, this is a basic feature to increase the quantity of information a single system is able to process.

Many authors refer to the number and variety of distinct behaviors, which are observed even in simple memristive circuits, as "extreme multistability" [22,23]. This property, however, has been mainly addressed via numerical simulations of artificial circuits, while real memristive devices are still affected by technological limitations, such as the operative ranges, which depend on the materials and the fabrication process. Nonetheless, in the recent works [27,28] real circuits with memristor have been investigated, verifying the richness of their dynamics. The digitalization of the ideal memristor has also been theorized as an alternative approach to overcome the implementation issues [29–31], but the research is still in a preliminary stage and no actual digital circuit mimicking the analog device has been produced yet.

Several analytic studies of circuits with ideal memelements have been recently presented with the goal of investigating the inner mechanisms responsible for the richness of the dynamics and the coexistence of many distinct regimes. The pioneering paper [16] has been the very first providing a mathematical explanation for the existence of multiple attractors in circuits with ideal memristors. The machinery behind this result is referred to as Flux-Charge Analysis Method [15], a technique developed to study circuits with memelements into their natural domain, i.e. the flux-charge representation of the devices. The application of this method generates an equivalent model of the circuit, where all the initial conditions of the memelements explicitly appear in the equations as coefficients. Therefore, the initial conditions of the system turn out playing the same role of tuning parameters, i.e. changing their values modifies the circuit dynamics. In general, the system is able to exhibit different behaviors just because of different initializations, a phenomenon also referred to as "bifurcations without parameters" [16,32]. The dynamics exhibited by circuits with ideal memristor can be also programmed by using a properly designed set of pulses, as illustrated in [33].

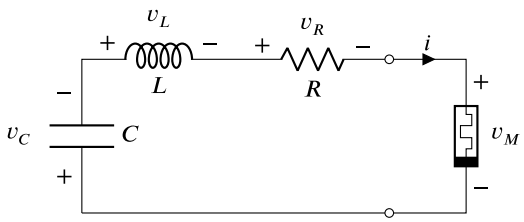

Fig. 1. The circuit studied in Section 2.1.

Inspired by Corinto and Forti [16], the problem of the coexistence of multiple attractors has been addressed in the domain of the original state variables in [34,35]. The results presented in these works refer to circuits with ideal memelements, whose presence causes the split of the state space into a continuum of manifolds, which turn out to be invariant with respect to the circuits dynamics, i.e. if the system is initialized onto a certain manifold, then the ensuing trajectory is bound to remain over there. The state space is also said to be "foliated" into infinitely many multidimensional surfaces. Conditions for the existence of this structure as well as a method to derive the mathematical form of the dynamics actually exhibited onto each invariant manifold have been provided. An important consequence of these results is that a circuit with ideal memelements can be completely studied in its natural domain using just the manifold dynamics, which is described by a reduced order model whose derivation requires some algebraic operations involving suitable changes of coordinates.

In this paper, we propose a new way for explaining the coexistence of multiple attractors and the extreme multistability seen in circuits with memristors. The mathematical tool that will be used is the concept of "first integral of the motion" [36], which is a relationship among the state variables that is constant along each solution of the circuit. It will be shown that the existence of a first integral is a common feature for a vast class of circuits featuring an ideal memristor, and that generalizations to the case of, even multiple, ideal memelements are straightforward. For these systems the first integral of the motion can always be written as a nonlinear differential equation of the memristor internal state, and so, in a sense it describes the evolution of the circuit as it is seen from the memristor point of view. Notably, this differential equation has order lower than the original model, and, above all, it is not autonomous, i.e. it describes a forced dynamics. The nature of the forcing input will be completely disclosed, because it turns out to be crucial in the analysis of the dynamics induced by a broader class of non-ideal memristive devices, which will be introduced later in this paper. Indeed, when the "ideality" is lost, the first integral of the motion disappears and thus the related differential equation no longer holds. Nevertheless, the circuit dynamics is still affected by the first integral since it obeys a structure where the previous nonlinear differential equation is no longer alone, but it interacts with other elements in a feedback interconnected fashion.

Hereafter, an example will be used to illustrate the computation of the first integral in a very simple circuit with an ideal memristor. The nonlinear differential equation obtained this way will also be used to infer some features of the overall dynamics.

2.1. Example: Resistor, capacitor, inductor, and q-memristor mesh

Consider a mesh featuring a resistor, a capacitor, an inductor, and an ideal charge-controlled memristor as depicted in Fig. 1, where

the value i represents the mesh current, while the voltages are taken according to the passive sign convention. Using the notation introduced in the figure, the resistor, capacitor and inductor are respectively described by the constitutive equations

$$v_R = Ri \ , \quad \frac{d}{dt}v_C = \frac{1}{C}i \ , \quad \frac{d}{dt}i = \frac{1}{L}v_L \ ,$$

and so the Kirchhoff voltage law yields the second order model

$$\begin{cases} \frac{d}{dt}v_C = \frac{1}{C}i \\ \frac{d}{dt}i = -\frac{1}{L}v_C - \frac{R}{L}i - \frac{1}{L}v_M \end{cases} . \tag{1}$$

Instead, the ideal charge-controlled memristor is modeled by

$$\begin{cases} \frac{d}{dt}q_M = i \\ v_M = G_{mr}(q_M)i \end{cases} , \tag{2}$$

where $G_{mr}(\cdot)$ is its memristance and q_M its charge. Notice that the combination of Eqs. (1) describing the linear part of the system and Eqs. (2) of the memristor provides the standard third-order autonomous model of the circuit. Next, we will illustrate that spotting a first integral in such a representation will lead to an equivalent but externally forced reduced order model.

Observe that

$$i = C\frac{d}{dt}v_C = \frac{d}{dt}q_M \ , \tag{3}$$

which implies that

$$\frac{d}{dt}\left(Cv_C - q_M\right) = 0 \ .$$

Integrating this equation, a first integral is finally discovered, and its form is

$$v_C = \frac{1}{C}q_M + w_0 \ , \tag{4}$$

where

$$w_0 = v_C(0) - \frac{1}{C}q_M(0) \in \mathbb{R} \tag{5}$$

with $v_C(0)$ and $q_M(0)$ denoting the initial conditions of the capacitor and the memristor. According to (3), i depends on q_M, while equation (4) implies that the knowledge of both w_0 and $q_M(t)$ for $t \geq 0$ provides the value of $v_C(t)$ for every $t \geq 0$. Therefore, these relationships can be exploited in the Kirchhoff voltage law along the mesh to obtain v_L as a function of q_M and w_0:

$$v_L = -\frac{1}{C}q_M - w_0 - R\frac{d}{dt}q_M - G_{mr}(q_M)\frac{d}{dt}q_M \ . \tag{6}$$

Then, using the constitutive equation of the inductor and Eq. (3), after properly arranging all the terms, we arrive to the following forced second order nonlinear differential equation

$$-\left(L\frac{d^2}{dt^2} + R\frac{d}{dt} + \frac{1}{C}\right)q_M - G_{mr}(q_M)\frac{d}{dt}q_M = w_0 \ , \tag{7}$$

which describes the dynamic behavior of the memristor charge q_M generated by the constant forcing term w_0.

Observe that Eq. (7) is equivalent to a second order system of ordinary differential equations. Indeed, using Eq. (3) it can be formulated as

$$\begin{cases} \frac{d}{dt}i = -\frac{R}{L}i - \frac{1}{LC}q_M - \frac{1}{L}G_{mr}(q_M)i - \frac{1}{L}w_0 \\ \frac{d}{dt}q_M = i \end{cases} \tag{8}$$

that is just a different way to represent Eqs. (3) and (6). System (8) describes the dynamics for initial condition that satisfy (5), and it is equivalent to (1) and (2) under the same initial configuration. In the third order model, however, the dynamics always satisfies (5), which means that the trajectory lies on a plane.

It is worth stressing that Eq. (7) depicts the circuit using a reduced order model which is parameterized by the initial conditions that modulate the forcing term w_0 according to (5). In other words, the first integral allows us to describe the circuit dynamics using a set of simplified models whose parametric configurations are related to the initial conditions. Moreover, the reduced order dynamics is taken from the perspective of the memristor itself, in the sense that it is expressed only through the variable q_M. The main advantage of (7) is that it has gained parameter w_0 to lose one degree in the model order, which otherwise would had been three.

The order reduction can deeply simplify the circuit analysis, as illustrated hereafter. From (7) it follows that all the equilibrium points of the circuit are solutions of

$$-\frac{1}{C}q_M = w_0$$

for $w_0 \in \mathbb{R}$. Notice that the corresponding value of v_C is zero, because the fixed point itself lies onto the first integral (see (4)). Moreover, the constitutive equations of both the capacitor and the memristor imply that in a steady regime the current must be equal to zero too. So, the equilibrium points have the form $(q_{Me}, v_{Ce}, i_e) = (-Cw_0, 0, 0)$, and since w_0 can sweep all the real values, they are not isolated and describe an infinite straight line. Their stability can be studied linearizing the parametric reduced order model (8) around the fixed points line $(i_e, q_{Me}) = (0, -Cw_0)$.

To clarify the circuit behavior, assume that

$$G_{mr}(q_M) = m_1 + 3m_3q_M^2 \ .$$

Then, the jacobian matrix reads

$$J(i, q_M) = \begin{bmatrix} -\frac{R + m_1 + 3m_3C^2w_0^2}{L} & -\frac{1}{LC} \\ 1 & 0 \end{bmatrix}$$

and, assuming $R, L, C > 0$, a fixed point $(i_e, q_{Me}) = (0, -Cw_0)$ is stable if

$$R + m_1 + 3m_3C^2w_0^2 > 0 \ .$$

If we set $m_3 > 0$ and $m_1 < -R$, then the stability depends on the condition

$$w_0^2 > -\frac{R + m_1}{3m_3C^2} > 0 \ ,$$

which means that for initial conditions such that w_0 in (5) satisfies this inequality a stable fixed point is experienced. Moreover, if $L > C\left(R + m_1 + 3m_3C^2w_0^2\right)^2$, at

$$w_0^2 = -\frac{R + m_1}{3m_3C^2} \tag{9}$$

a Hopf bifurcation "without parameters" occurs (see [37] and references therein), and, therefore, somewhere in the range

$$|w_0| < \sqrt{-\frac{R + m_1}{3m_3C^2}} \ ,$$

limit cycles appear, as much probably as they are close to the bifurcation onset. Notably, many of the above computations have been made easier thanks to the simplified parametric model (7) (or equivalently (8)) being second order.

Summing up, for proper choices of the circuit parameters, we can witness quite a complex behavior. Indeed, given an initial configuration of the circuit, let it be $(q_M(0), v_C(0), i(0))$, if

$$\left|v_C(0) - \frac{1}{C}q_M(0)\right| > \sqrt{-\frac{R + m_1}{3m_3C^2}} \ ,$$

the circuit evolves towards a fixed point at $(-Cv_C(0) - q_M(0), 0, 0)$. Otherwise, limit cycles are expected to appear near the Hopf bifurcation (9).

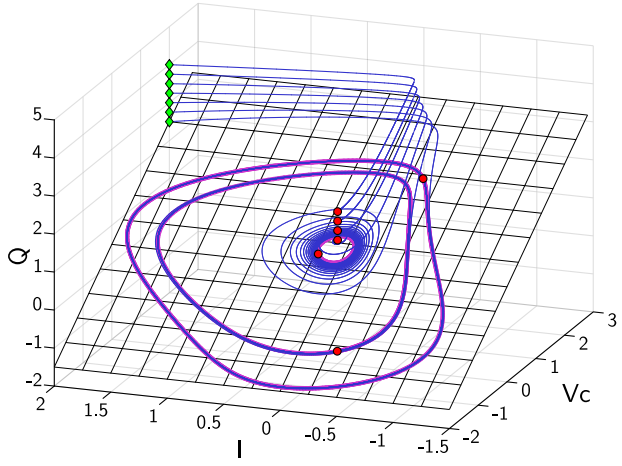

Fig. 2. Orbits of the circuit analyzed in Section 2.1. All the trajectories have been initialized for the same couple $(v_C, i) = (2, 2)$, but different values of q_M (green diamonds). The final points reached by the simulations are marked with red circles. Different regimes (purple lines) are exhibited by the selected orbits. In particular, attractive fixed points and attractive limit cycles are reached after the transients. According to (4) and (5), each trajectory evolves on a different plane of the form $v_C - \frac{1}{C} q_M = w_0 = v_C(0) - \frac{1}{C} q_M(0)$. One of them has been depicted with a wired surface. (For interpretation of the references to color in this figure legend, the reader is referred to the web version of this article.)

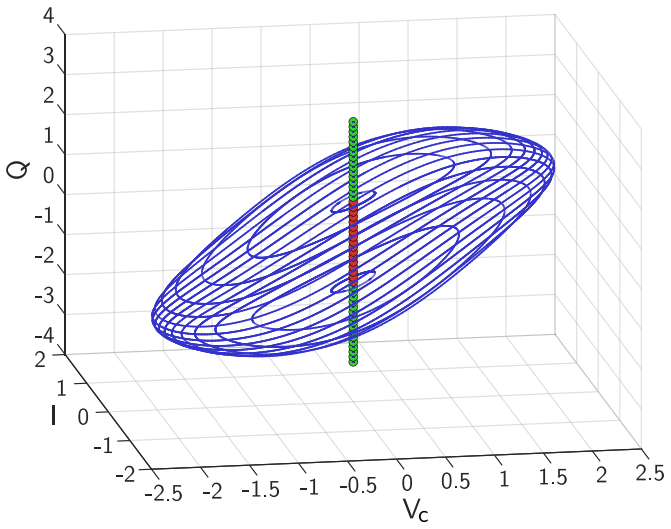

Fig. 3. Solutions of the circuit studied in Section 2.1. The blue curves are the regime orbits obtained initializing the circuit on different first integrals. As one can imagine, the system has a continuous envelope of limit cycles, a case of coexistence of attractors which boils down to "extreme multistability." The circuits has also an infinite number of fixed points arranged along a straight line. The green circles are fixed points, which are "transversally" attractive with respect to that line, while the red circles denote "unstable" fixed points. (For interpretation of the references to color in this figure legend, the reader is referred to the web version of this article.)

Consider the following configuration in normalized units of measure

$$R = 1\ ,\ L = 2\ ,\ C = 1\ ,\ m_1 = -2\ ,\ m_3 = 1/3\ ,$$

which yield $\sqrt{-(R+m_1)/(3m_3C^2)} = 1$. In Fig. 2 seven trajectories starting from the same $(v_C(0), i(0))$, but for different values of $q_M(0)$, are depicted. The initial conditions of the charge are chosen to span over both the side of the Hopf bifurcation. The figure shows the coexistence of attractors. Indeed, depending on the initialization, the trajectory converges to a fixed point, with different transients, or to a limit cycle. In Fig. 3 a greater number of initial conditions spanning an interval larger than the condition for the existence of limit cycles has been considered. The figure only shows the regime behavior, thus highlighting the existence of an infinite number of coexisting attractors.

3. First integral equations in circuits with an ideal memristor

The situation presented in the previous example of Section 2.1 is not a special case. In fact, hereafter, we will develop a technique to prove the structural existence of a first integral in circuits with an ideal memristor. Moreover, we will show that the first integral is naturally associated to a non-homogeneous nonlinear differential equation of reduced order with respect to the original dynamics in the memristor state variable, and that the forcing input turns out to be a constant signal depending on the initial conditions. Such a signal will play a crucial role in Section 6, where we will extend the proposed analysis tools to non-ideal memristive devices. Moreover, it will be highlighted that the constant forcing input spans over the entire real axis, according to the nature of the memristor characteristic function, and that this feature is the key for the coexistence of a possibly infinite number of attractors in the state space of circuits of the class introduced hereafter.

Let Σ be a one port circuit containing only linear elements of any kind, except for independent voltage and current sources, which are excluded only for the sake of simplicity. The circuit is depicted in Fig. 4, where an ideal memristor is connected to the port of Σ. Extensions to different ideal memelements and to multi-port versions of circuit Σ are straightforward, and they will be shortly discussed in the next section.

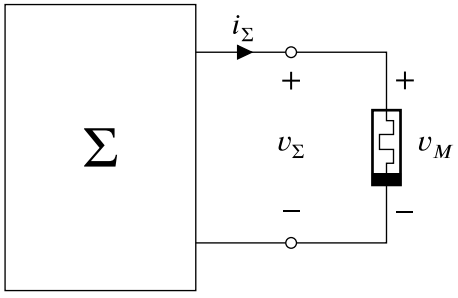

Fig. 4. Schematics of a circuit featuring only one memristor. The memristor is isolated, so that the remaining part of the circuit can be addressed as a one-port device connected to it.

Denote the voltage of Σ measured between the terminals of its port as v_Σ, and let i_Σ be the related current, taken using the active sign convention. Under the previous assumptions, circuit Σ enforces a relationship between v_Σ and i_Σ, which involves multiple derivatives and polynomial rules. To be precise, if we denote the derivative operator as

$$\mathcal{D} = \frac{d}{dt}\ ,$$

such a relationship can be formulated as

$$\Gamma_v(\mathcal{D}) v_\Sigma(t) = \Gamma_i(\mathcal{D}) i_\Sigma(t)\ ,$$

where $\Gamma_v(\cdot)$ and $\Gamma_i(\cdot)$ are assumed to be coprime polynomials. Notice that the relative order between Γ_v and Γ_i defines the causality of Σ: If the degree of Γ_v is strictly higher than that of Γ_i, then Σ induces a strictly causal relationship from i_Σ to v_Σ, and vice versa. When their degree is just the same, the relationship is causal, but not strictly, from both the directions.

Since we want to deal with causal operators, let us introduce the following notation. Denote as $Q(\mathcal{D})$ the polynomial with higher (or, at most, equal) degree between $\Gamma_v(\mathcal{D})$ and $\Gamma_i(\mathcal{D})$, and let $P(\mathcal{D})$ represent the other one. If P is Γ_v, then let u denote v_Σ, and y the current i_Σ. Otherwise, let u represent i_Σ, and u the voltage v_Σ. Hence, the causal

relationship described by circuit Σ can be expressed as

$$y(t) = \frac{P(D)}{Q(D)}u(t) = L(D)u(t) \ ,$$

where Q has degree n and P degree $m \leq n$. Notice that the two polynomials can always be rewritten in the form

$$P(D) = b_m D^m + b_{m-1} D^{m-1} + \cdots + b_1 D + b_0 \ ,$$
$$Q(D) = D^n + a_{n-1} D^{n-1} + \cdots + a_1 D + a_0 \ .$$

We also enforce the working hypothesis $Q(0) = a_0 \neq 0$, which prevents $L(D)$ from exhibiting a native integral effect.

Consider now the ideal memristor connected to Σ, and assume for this device the passive sign convention. The memristor equations, then, reads

$$\begin{cases} Dx = y \\ u = G(x)y \end{cases} \ . \tag{10}$$

The state variable x can alternatively be q_M or φ_M depending on the memristor being charge- or flux-controlled. Notably, the nature of Σ can restrict the types of memristor that can be connected to it. In particular, observe that x is equal to the flux φ_M, if y is v_Σ, while x is the charge q_M, when y is i_Σ. Therefore, if Σ is strictly causal, the nature of x and y is uniquely fixed and only one kind of ideal memristor can be connected to it. Otherwise, if Σ is causal, but not strictly, v_Σ and i_Σ can be switched in the role of x and y, and so both the flux-controlled and the charge-controlled memristor can be used. Assume that the nonlinear characteristic $G(\cdot)$ is the derivative of a function $H(\cdot)$, so that

$$u = G(x)y = DH(x) \ .$$

Function H must be differentiable a sufficient number of times to satisfy the consistency of the model. Hence, the complete circuit dynamics is described by

$$y - L(D)DH(x) = y - \frac{P(D)}{Q(D)}DH(x) = 0 \ . \tag{11}$$

Observe that $y = Dx$, and recall that $Q(0) \neq 0$, so that also $Q(D)$ and D are coprime. Then, the application of the operator $Q(D)$ to both of the sides brings to

$$Q(D)Dx - P(D)DH(x) = 0 \ , \tag{12}$$

which is a nonlinear homogeneous differential equation of degree $n+1$ in x, i.e. it can be formulated as

$$\mathcal{F}\left(D^{n+1}x, D^n x, \dots, Dx, x\right) = 0 \tag{13}$$

for some proper function $\mathcal{F} : \mathbb{R}^{n+2} \to \mathbb{R}$. Notice that the solutions of such an equation are described by trajectories in a $(n+1)$-dimensional state space. A common choice for the state space is

$$\mathcal{S} = \left\{(x, Dx, \dots, D^n x)^T \in \mathbb{R}^{n+1}\right\} \ . \tag{14}$$

Such a space can be used only if the operator $P(D)DH(\cdot)$ is well-posed, that depends on the regularity of the nonlinearity $H(\cdot)$. In the end the condition for $\mathcal{S}$ being a proper state space is just an extension of the one making the memristor model consistent, and that is why this choice is so widespread. Then, in the rest of the paper $\mathcal{S}$ will always be assumed as in (14). Notice that the variables of $\mathcal{S}$ may not represent electric quantities strictly related to the single elements of the circuit. Nonetheless, if Σ is a properly defined circuit, it always exists a linear invertible transformation, that changes its natural state variables, i.e. the voltages of the capacitors and the currents of the inductors, into those of $\mathcal{S}$, and vice versa (see [34]).

Let us now integrate the differential equation (12) to compute its first integral. This is formally done by applying to both the sides the operator D^{-1}, which is defined as the inverse operator of D, i.e. the one satisfying

$$D^{-1}D = DD^{-1} = Id \ ,$$

where Id represents the identity operator. Since D and D^{-1} commute by assumption, Eq. (12) becomes

$$Q(D)x - P(D)H(x) = w \ ,$$

where w is a signal satisfying

$$Dw(t) = 0 \ .$$

Therefore, it is straightforward to verify that $w(t) = w_0$, $w_0 \in \mathbb{R}$, for all t. This makes the above equation equal to

$$Q(D)x - P(D)H(x) = w_0 \tag{15}$$

that is a first integral of the dynamics, because it involves the variable x and at most its first n derivatives, i.e. it defines a constant relationship among the state coordinates of the space $\mathcal{S}$. Indeed, Eq. (15) can be rewritten in the form

$$\Omega\left(D^n x, \dots, Dx, x\right) = w_0 \tag{16}$$

for some proper nonlinear function $\Omega : \mathbb{R}^{n+1} \to \mathbb{R}$ acting as a structural condition each trajectory in $\mathcal{S}$ has to satisfy always and everywhere. Eq. (16) is also connected to the existence of invariant manifolds in the circuit state space (see [34]).

Notably, the first integral (15) also represents a nonlinear non-homogeneous (or forced) differential equation of degree n in the variable x. The "artificial" input w_0 is constant, and its value deeply affects the dynamics actually exhibited by the circuit. Varying w_0 modifies its behavior, for instance, by changing the displayed attractor.

Eq. (15) is a first integral of the motion, and it also describes the dynamics of the complete circuit. Consequently, a reduced order model in the coordinates $(x, Dx, \dots, D^n x)$ and parametric in the initial configuration through w_0 is sufficient to represent the whole system. Such a model reduction turns out to be a powerful tool for the circuit analysis, as it will be illustrated in Sections 3.2, 3.3, and 3.4.

3.1. Technical remarks and extensions

In this section a number of technical observations will be provided to highlight how the first integral affects the inner structure of the system dynamics, and to stress the role of the elements it is made up of.

First, notice that the first integral exists because

$$Q(D)Dx - P(D)DH(x) = 0 \xrightarrow{D^{-1}} Q(D)x - P(D)H(x) = w_0 \in \mathbb{R}$$

means that

$$\mathcal{F}\left(x, Dx, \dots, D^n x, D^{n+1}x\right) = 0 \xrightarrow{D^{-1}} \Omega\left(x, Dx, \dots, D^n x\right) = w_0 \in \mathbb{R}$$

in the $(n+1)$-dimensional space $\mathcal{S}$, where (16) is an invariant manifold. Therefore, the same space $\mathcal{S}$ is just where the features induced by the first integral take form and become evident. Moreover, since Eq. (15) describes the whole system through a reduced order model in the coordinates $(x, Dx, \dots, D^n x)$, there exists a mapping from the natural variables of the circuit and $\mathcal{S}$. As a byproduct, the initial configurations at $t = 0$ of both Σ and the memristor translate into a certain $(x(0), Dx(0), \dots, D^n x(0))$, and so w_0 can be computed as

$$w_0 = \Omega\left(x(0), Dx(0), \dots, D^n x(0)\right) \ . \tag{17}$$

Notably, if, in addition to being sufficiently regular, $H(x)$ is also properly defined for all $x \in \mathbb{R}$, then for any $w_0 \in \mathbb{R}$ there exist initial conditions, i.e., $(x(0), Dx(0), \dots, D^n x(0))^T \in \mathbb{R}^{n+1}$, such that (17) holds, thanks to the assumption $m \leq n$ on the degrees of P and Q. Clearly, all the states belonging to the manifold defined by (16) share the same value of w_0.

Moreover, Eq. (16) also implies that w_0 acts as an "index" that selects which first integral of the motion is actually followed by the circuit dynamics. Therefore, since it plays the role of a forcing input

for the reduced order dynamics (15), it deeply affects the behavior exhibited along the first integral. If for different values of w_0 the forced nonlinear dynamics (15) exhibits distinct regimes, then the state space of the circuit comprises as many coexisting attractors. However, changing the index w_0 is not the only way to modify the regime. Indeed, for a fixed w_0 the reduced order nonlinear dynamics (15) can be multistable by itself, and therefore different initial conditions $(x(0), Dx(0), \dots, D^n x(0))^T \in \mathbb{R}^{n+1}$ related to the very same w_0 can converge to different attractors. Hence, always starting the circuits from the same w_0 may be not enough to uniquely determine its regime. This is a peculiar property that greatly increases the capability of the complete system to generate very rich and complex multistable scenarios.

The existence of the first integral of the motion has been proved for the simple circuit depicted in Fig. 2, but it can be proved in an analogous way even in far more complex configurations. Hereafter, an outline of the techniques to extend the previous results to more complicated circuits is presented.

The first extension consists in considering the same circuit structure, but substituting the ideal memristor with any other ideal memelement (see [34,38] for their mathematical modeling). In such a configuration, an analogous result about the existence of a first integral of the motion can be proved using a method almost identical to the previous one. So, our procedure turns out general with respect to any ideal memelement.

Another interesting extension is when Σ is a multi-port version of the circuit considered so far and many ideal memelements are connected to it. In this case we get a couple (u_i, y_i) for each port and $L(D)$ is replaced by a matrix of similar operators, leading to as many equations of the form (11) where each memelement adds its own contribution. Exploiting the constitutive equations of the memelements and properly collecting the D operator, the differential equations can be put in an integrable form. Then, since the port variable y_i possibly depend on all the u_i, there exist changes of coordinates which cast the complete dynamics into a single extended state space of minimal degree, where the previous first integrals of the motion merge into a unique higher order structure of invariant manifolds.

Circuit Σ can be extended to include voltage and current sources. In this case the analysis can be carried on the same way by pulling all the sources out of Σ and considering it as a multi-port connected to all of them and to the memelements. Then, after a proper rearrangement of the differential equations, all the contributions of the sources can be pushed to the right hand sides of otherwise homogeneous equation similar to (13). Hence, after the integration the forcing external inputs are not constant terms of the form w_0 any more, but they are time-varying signals depending on the sources. In this case the existence of the integrals of the motions depends on the sources, and in particular on their capability to keep these forcing external inputs constant. Nevertheless, if the sources can be modeled as the outputs of known autonomous models, then the explicit dependence on the time can be removed, and the first integral structure comes out again (see also [17]). From a different point of view, the dynamics in presence of sources can be seen as the ensemble of a state space foliated in invariant manifolds and a driving mechanism that forcibly makes the trajectory switch from one to another.

Using the same pushing out technique, similar results can be possibly derived even when other nonlinear electronic components, other than the memelements, are present in the circuit. Indeed, each of them can be modeled as connected to Σ through a dedicated port, and so its contribution appears as a port equation. For the sake of simplicity but without loss of generality, assume they do not add any other state variable. Then, their port equations just provide nonlinear relationships which add nonlinear contributions to the remaining equations having the form (12). Therefore, if they do not prevent collecting the derivative operator D, a first integral of the motion can be spotted again. This demonstrates how general the mechanism that generates the first integrals is, and justifies why their existence is very common in circuits with ideal memelements.

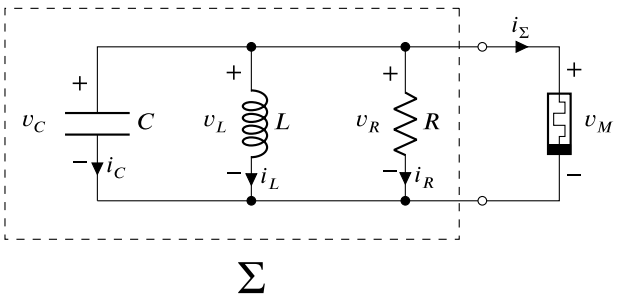

Fig. 5. The circuit illustrated in Section 3.2.

3.2. Example: Resistor, capacitor, inductor, and φ-memristor cut

Consider a circuit with a single cut consisting of a resistor, a capacitor, an inductor, and a flux-controlled memristor as in Fig. 5. Moreover, let R, C, and L be the resistance, capacitance, and inductance of the previous elements, which are all connected to the same two terminals, forming the circuit Σ as depicted in the figure. Denoting as v_Σ its voltage, straightforward computations lead to the sought input–output formulation of the circuit:

$$v_\Sigma = -\frac{\frac{1}{C}D}{D^2 + \frac{1}{RC}D + \frac{1}{LC}} i_\Sigma \ .$$

Then, in this case necessarily $y = v_\Sigma$, $u = i_\Sigma$, and

$$L(D) = \frac{-\frac{1}{C}D}{D^2 + \frac{1}{RC}D + \frac{1}{LC}} = \frac{P(D)}{Q(D)} \ .$$

The only memristor suitable to be connected to this Σ is the flux-controlled one, whose equations read

$$D\varphi_M = v_\Sigma \ .$$

For the sake of simplicity, let us enforce the hypothesis that the memconductance is an integrable function, i.e.

$$G_{mc}(\varphi_M) = \frac{\partial H_{mc}(\varphi_M)}{\partial \varphi_M} \ .$$

Therefore, it holds that

$$i_\Sigma = G_{mc}(\varphi_M) v_\Sigma = D H_{mc}(\varphi_M) \ .$$

Comparing this model with (15), it directly follows that $x = \varphi_M$. Hence, the sought first integral has the form

$$\left(D^2 + \frac{1}{RC}D + \frac{1}{LC}\right)\varphi_M + \frac{1}{C} D H_{mc}(\varphi_M) = w_0 \ .$$

Assume now that

$$H_{mc}(\varphi_M) = m_1 \varphi_M + m_3 \varphi_M^3 \ ,$$
$$G_{mc}(\varphi_M) = m_1 + 3 m_3 \varphi_M^2 \ .$$

Then, the first integral boils down to

$$D^2\varphi_M + \frac{1 + m_1 R}{RC} D\varphi_M + \frac{1}{LC}\varphi_M + \frac{3m_3}{C}\varphi_M^2 D\varphi_M = w_0 \ . \tag{18}$$

Since

$$D\varphi_M = v_\Sigma = v_C \ ,$$
$$D^2\varphi_M = Dv_C = \frac{1}{C} i_C = -\frac{1}{C}\left(G_{mc}(\varphi_M) v_C + \frac{1}{R} v_C + i_L\right) \ ,$$

the first integral can be represented in the natural state space (v_C, i_L, φ_M) of the circuit as

$$-\frac{1}{C}\left(m_1 v_C + 3 m_3 \varphi_M^2 v_C + \frac{1}{R} v_C + i_L\right)$$

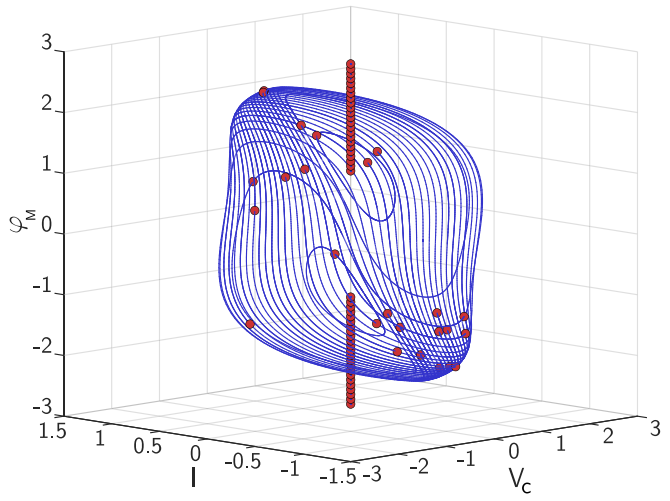

Fig. 6. Orbits of the circuit studied in Section 3.2, obtained initializing the system on different first integrals. The figure portrays only the regime trajectories. The ending points of the simulated solutions are marked with red circles. The situation illustrates the coexistence of infinitely many attractors in the forms of limit cycles and fixed points. (For interpretation of the references to color in this figure legend, the reader is referred to the web version of this article.)

$$+\frac{1+m_1R}{RC}v_C+\frac{1}{LC}\varphi_M+\frac{3m_3}{C}\varphi_M^2v_C=w_0$$

which boils down to the 2-dimensional invariant manifold:

$$\varphi_M-Li_L=LCw_0\ .$$

Fig. 6 depicts the regimes reached for different values of w_0, when for the circuit configuration in normalized units of measure is

$$R=1\ ,\ L=2\ ,\ C=1\ ,\ m_1=-2\ ,\ m_3=\frac{1}{3}\ .$$

The admissible values of w_0 are infinite, since $w_0\in\mathbb{R}$, and, indeed, the exhibited attractors count not isolated fixed points, as well as not isolated limit cycles as shown in Fig. 6. The circuit, then, displays "extreme multistability," in the sense that it has an infinite number of coexisting not isolated attractors of various nature.

It is worth stressing that this infinite structure of attractors has been spotted thanks to the reduced order model (18) that is parametric in the initial configuration of the circuit. Then, the existence of a first integral of the motion and the corresponding capability of describing the dynamics in terms of trajectories evolving onto invariant manifolds are powerful tools for the analysis of these kind of circuits. The implications of the peculiar results found in this example will be investigated in the next section for the entire class of circuits with ideal memelements featuring first integrals of the motions.

3.3. Coexistence of attractors and extreme multistability reloaded

According to the theory developed so far, the behavior of a circuit with an ideal memristor is completely described by a reduced order dynamics, that describes how it evolves, as it is seen from the memristor point of view. Notably, the reduced order model is a nonlinear non-homogeneous differential equation of the state variable of the memristor, and it turns out to be just the first integral of the trajectory. The forcing input is a constant signal depending exclusively on the initial conditions of the circuit, and it is crucial in defining the actual motion exhibited by the system in the state space. In fact, it strongly affects the dynamics, as it is capable of changing the number and the nature of the attractors revealed by the circuit regime. In this perspective, the forcing input acts as a tuning parameter, but it is more precise to consider it just as the index of the actual first integral. Indeed, different initial conditions can cast the circuit on the same first integral, but this latter can be made of several distinct trajectories, and, therefore, the one actually exhibited by the system depends on the starting point.

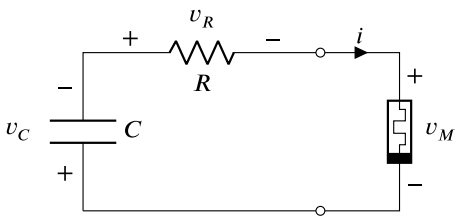

Fig. 7. The elementary circuit illustrated in Section 3.4.

The behaviors associated to the each first integral are distinct, because the related forcing input alters the layer where the solutions of the reduced order dynamics are confined to lie. Moreover, each first integral is a unique composition of trajectories with their own nature. For instance, as already observed in the previous examples, the same system can reveal a steady state, when initialized on a certain first integral, and a limit cycle when it is started on a different one, but this situation can occur even within the same first integral. Hence, the possible regime, and so the attractor, reached by the complete circuit is strictly dependent on the initial conditions, which define not only the first integral of the motion, but also the exact trajectory over it. Therefore, the number of the possible attractors, which exist under the same circuit configuration, is tied to the regimes reached by the reduced order non-homogeneous differential equation as the constant forcing input w_0 varies. See also Sections 3.1 and 3.2, where this scenario has already been underlined.

When the system has an infinite continuum of attractors, they can be scanned just by varying the initial conditions, and, since they are not bound to share the same nature, one can pass from a type to another as the initialization is varied, provided that the first integral index is changed, as well. This scenario is exactly what is called "bifurcation without parameters" [16,32], and it is the main ingredient for the "extreme multistability" recipe. Indeed, this latter is nothing more than a situation, where in neighboring first integrals reside different, and possibly complicated, attractors, such as chaotic attractors with different scroll structures.

Then, the coexistence of multiple attractors in a broad class of circuits with ideal memelements is a structural property, and not a special case. In particular, the infinite continuum of attractors, which forms the extreme multistability exhibited by several examples in the literature, depends only on the nature of the nonlinear characteristic of the memelements, that, nonetheless, provides such a situation under very mild conditions.

In the next section an example will be used to illustrate the structure of the first integrals of a circuit with a memristor, and how the dynamics is affected by the stable and unstable solutions on them.

3.4. Example: Resistor, capacitor, and φ-memristor mesh

Consider a simplified version of the circuit studied in Section 2.1, i.e., a mesh featuring a resistor, a capacitor, and an ideal flux-controlled memristor as depicted in Fig. 7. Let i be the mesh current, and assume the passive sign convention for the voltages. The sought circuit Σ consists of the series of a resistor with resistance R and a capacitor with capacitance C. Taking $i_\Sigma=i$ and $v_\Sigma=v_M$ to follow the same procedure used so far, the corresponding input–output model assumes the form

$$i_\Sigma=CDv_C=CD(-v_\Sigma-v_R)=-CD(v_\Sigma+Ri_\Sigma)$$

which boils down to

$$i_\Sigma = -\frac{CD}{CRD+1} v_\Sigma \ .$$

The model of the ideal flux-controlled memristor with memconductance $G_{mc}(\cdot)$ reads

$$\begin{cases} D\varphi_M = v_M \\ i_M = G_{mc}(\varphi_M) v_M \end{cases} \ , \tag{19}$$

where φ_M is the memristor's flux and $i_M = i$. Therefore, $y = v_\Sigma$ and $u = i_\Sigma$, which imply that

$$L(D) = -\frac{CRD+1}{CD} = \frac{RD + \frac{1}{C}}{D} = \frac{P(D)}{Q(D)} \ .$$

Notice that the relative degree of $L(D)$ is zero, and so circuit Σ can finely work with a charge-controlled memristor too.

We also assume that the memconductance $G_{mc}(\cdot)$ is an integrable function, and we denote its integral as $H_{mc}(\cdot)$, so that

$$DH_{mc}(\varphi_M) = \frac{d}{dt} H_{mc}(\varphi_M) = \frac{\partial H_{mc}(\varphi_M)}{\partial \varphi_M} \frac{d\varphi_M}{dt} = G_{mc}(\varphi_M) v_M = i \ .$$

The first integral (15) becomes

$$Dx - RDH_{mc}(x) - \frac{1}{C} H_{mc}(x) = w_0 \ , \tag{20}$$

where $x = \varphi_M$. Notice that $Dx = D\varphi_M = v_M = v_\Sigma$ and $RDH_{mc}(\varphi_M) = Ri = v_R$. So it follows that (20) boils down to

$$v_C - \frac{1}{C} H_{mc}(\varphi_M) = w_0 \tag{21}$$

for some constant w_0 whose actual value can be computed from the circuit initial conditions as

$$w_0 = v_C(0) - \frac{1}{C} H_{mc}(\varphi_M(0)) \ .$$

It is worth stressing that the first integral (20) is a geometric locus, where the system state is bound to remain after the initialization.

The existence of the first integral has important consequences for the circuit dynamics, because the natural state variables are not independent, but they are tied together. For instance, in this case, the value of v_C depends on that of φ_M, given the circuit initialization represented by w_0, i.e., the trajectories move along 1-dimensional manifolds in $\mathbb{R}^2$. Hence, to describe the circuit behavior it is sufficient to study the evolution of φ_M. In order to reduce the complete dynamics to that of φ_M only, derive v_M from the Kirchhoff voltage law and use it into the second constitutive equation of the memristor to obtain

$$i = G_{mc}(\varphi_M)(-v_C - Ri) \ .$$

Hence, excluding the special case $1 + RG_{mc}(\varphi_M) = 0$ where the solution is forced at $v_C = 0$, in general it holds true that

$$i = -\frac{G_{mc}(\varphi_M)}{1 + RG_{mc}(\varphi_M)} v_C \ . \tag{22}$$

Then, the first constitutive equation of the memristor becomes

$$D\varphi_M = -v_C - Ri = -v_C + \frac{RG_{mc}(\varphi_M)}{1 + RG(\varphi_M)} v_C = -\frac{H_{mc}(\varphi_M) + Cw_0}{C\left(1 + RG_{mc}(\varphi_M)\right)} \ .$$

Hence, from the evolution of φ_M alone, we get the complete behavior of the circuit thanks to (21).

The existence of the first integral provides remarkable simplifications in the analysis of the dynamics, which has been reduced to just a single first-order differential equation. To begin with, observe that any value φ, satisfying $H_{mc}(\varphi)/C + w_0 = v_C = 0$, also implies that $\frac{d}{dt}\varphi_M = 0$. Therefore, the circuit has as many equilibrium points, as the solutions of this condition for w_0 spanning the real axis. Then, the fixed points always have the form $(\varphi_M = \varphi, v_C = 0)$ for any proper value of φ, which implies that, depending on the nature of $H_{mc}(\varphi)$, they can be not isolated.

The analysis of the system trajectories turns out simplified as well. Remember, that in the state space (φ_M, v_C) the trajectories are bound to stay on their first integral, i.e. they satisfy $v_C = H_{mc}(\varphi_M)/C + w_0$, where w_0 is fixed by the initial conditions of the circuit. Then, the first integral is a curve swept according to the sign of $D\varphi_M$, or equivalently the sign of

$$\frac{H_{mc}(\varphi_M) + Cw_0}{1 + RG_{mc}(\varphi_M)} \ . \tag{23}$$

When the sign of (23) is positive, the trajectory moves along the first integral in the direction of the negative values of φ_M, and towards the positive ones otherwise.

Notice that depending on the form of $H_{mc}(\cdot)$ and on the value of w_0, the graph of curve (20) may pass through one or more equilibrium points, which will divide it into branches. Therefore, a first integral can be a single trajectory as well as the ensemble of several trajectory connected by fixed point, i.e., heteroclinic orbits [39]. Since the ending point of each branch can be different or it could even be at the infinity, the regime exhibited by the circuit not only depends on the first integral where it has been initialized, but also on the specific point on it.

To fix the ideas, assume that

$$H_{mc}(\varphi_M) = m_1 \varphi_M + m_3 \varphi_M^3 \ , \tag{24}$$

$$G_{mc}(\varphi_M) = m_1 + 3m_3 \varphi_M^2 \ . \tag{25}$$

Since the initial conditions $\varphi_M(0)$ and $v_C(0)$ can be any real value, also the first integral constant does so, i.e. $w_0 \in \mathbb{R}$. Therefore, the fixed points are represented by the couples $(\varphi_M = \varphi, v_C = 0)$, where φ satisfies

$$m_1 \varphi + m_3 \varphi^3 + Cw_0 = 0$$

as w_0 sweeps all the real values. Roughly speaking, the equilibrium points are given by the intersections of a cubic function of φ with the axis $v_C = 0$. It is straightforward to check that $\varphi \in \mathbb{R}$, which implies that all the axis $v_C = 0$ is made of not isolated fixed points. Moreover, it is worth observing that any first integral is the ensemble of different trajectories. Indeed, assume the circuit is initialized so that $v_C(0) - H_{mc}(\varphi_M(0))/C = w_0$. Then, the system state evolves on $v_C - H_{mc}(\varphi_M)/C = w_0$, whose intersections with the axis $v_C = 0$ are fixed points (one or three), while the branches obtained by these cuts are curves (two or four branches), where the state evolves according to the sign of

$$\frac{m_1 \varphi_M + m_3 \varphi_M^3 + Cw_0}{1 + m_1 R + 3m_3 R \varphi_M^2} \ .$$

Notice that, if $R > 0$, $m_3 > 0$ and

$$-\frac{1}{R} < m_1 < 0 \ ,$$

then, the previous condition reduces to evaluate the sign of

$$m_1 \varphi_M + m_3 \varphi_M^3 + Cw_0 \ ,$$

that is clearly related to the first integral (21).

Fig. 8 depicts the layered structure of the trajectories in the plane (φ_M, v_C), highlighting some first integrals and assuming that the circuit is configured according to the following parameters in normalized units of measure:

$$R = 0.5 \ , \ C = 2 \ , \ m_1 = -1 \ , \ m_3 = 1/3 \ . \tag{26}$$

The trajectories above the axis $v_C = 0$ are swept from the right to the left, while the state move in the opposite direction on those below. Observe that the fixed points on $v_C = 0$, whose coordinate φ_M belongs to $(-\infty, -1) \cup (1, \infty)$, are "transversally" stable, because the trajectories approach them asymptotically following the first integrals. It is worth stressing that this feature is an orbital stability property, because any perturbation "transverse" to the first integral curve is never absorbed back. The equilibrium points with $\varphi_M \in (-1, 1)$, instead, are "transversally" unstable, because two branches of the first integral diverge from them.

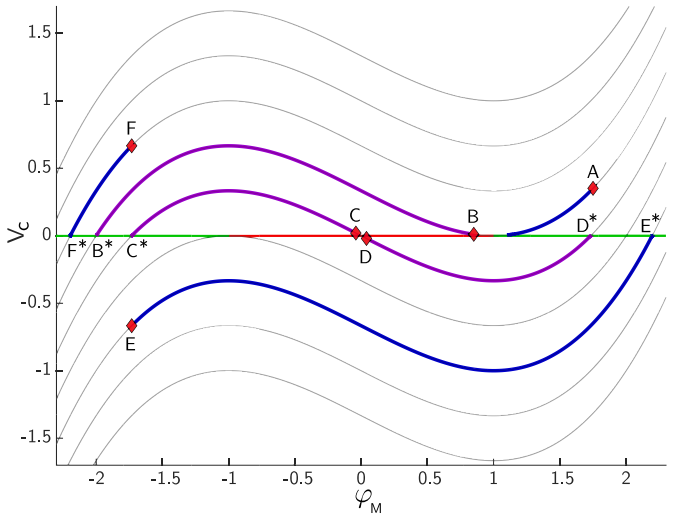

Fig. 8. Trajectories portrait of the circuit illustrated in Section 3.4 and depicted in Fig. 7. The "s"-shaped gray curves are examples of first integrals. Their intersections with the horizontal axis $v_C = 0$ provide the fixed points. Since the solutions move from right to left on the upper semi-plane, and from left to right otherwise, the fixed points on the green branches are always approached in an attractive manner, while those on the red ones are unstable to local perturbations. The red diamonds represent the starting points of the portrayed trajectories. The purple solutions are heteroclinic orbits. (For interpretation of the references to color in this figure legend, the reader is referred to the web version of this article.)

4. Energetic characterization of ideal memristors

In this section we investigate the energetic behavior of circuits with an ideal memristor in the light of the previous discussion on their first integral. Such an insight turns out necessary, because the structural existence of a first integral makes the circuits with ideal memristors very close to Hamiltonian systems (see, .g., [40]), where the first integral is usually caused by a conservation law, often related to the energy. So, we believe a further investigation of what is conserved in an ideal memristor circuit is important as much as its energetic characterization.

To this aim, consider the circuit of Section 3.4 as an example. First, observe that according to the standard definition the resistor is passive, while the capacitor is reactive. About the memristor, instead, the situation is more complicated. Indeed, parameters (26) make memconductance (25) negative for $\varphi_M \in (-1, 1)$, so that the second constitutive equation of memristor model (19) implies

$$i_M v_M = G_{mc}(\varphi_M) v_M^2 \ , \tag{27}$$

which describes energy absorption when $\varphi_M \in (-\infty, -1) \cup (1, \infty)$, and energy generation for $\varphi_M \in (-1, 1)$. An element featuring such a behavior is often referred to as "locally active," and its implementation requires an embedded generator. Then, it is important to ascertain which kind of relationship the memristor can set up with the other elements, and if there is evidence of a phenomenon such as energy storage.

Let us consider the following experiments. For starters, initialize the circuit in $(\varphi_M, v_C) = (1, 0)$. Since it is a fixed point, the circuit will exhibit a steady state response. Then, let us perturb this initial condition increasing φ_M over 1 by a small quantity, but remaining onto the first integral passing for that same equilibrium point. Denote the new initial condition as A, see Fig. 8. According to the circuit dynamics, the solution evolves along its first integral, and the dynamics of Dv_C is such that the system proceeds backwards to the previous fixed point. So, this perturbation along the first integral of the motion caused the displacement to be reabsorbed into the original steady state. However, if the perturbation along the same first integral starts from a φ_M lower than 1, namely B in the figure, even for arbitrary small displacements, the solution evolves towards the steady state marked as B*. Notice that the different behavior is due the initialization on two distinct branches of the first integral, which have different ending points. In particular, the second branch from B to B* is a heteroclinic orbit.

Consider now a similar experiment, but performed around the fixed point in $(\varphi_M, v_C) = (0, 0)$. As before, let us perturb the equilibrium along the first integral using two different displacements, one for each side of the steady state. The corresponding starting points are marked in Fig. 8 as C and D. When the circuit is initialized in C, it moves towards lower values of φ_M and it eventually lands in $(-1.732, 0)$. Conversely, when the initial condition is set in D, the solution moves for higher values and it finally reaches $(1.732, 0)$. Hence, the exhibited behavior is very different depending on the side the perturbation is applied to.

The above experiments underline that the first integral is in general split into branches separated by fixed points characterized by non trivial stability features, as for the "saddle" and the "unstable" equilibria above. Some of these branches, for instance, are heteroclinic orbits. Then, as already highlighted, the first integral is not a "single entity" with a unique dynamical characterization, but, rather, several kinds of trajectories can be embedded into it, each one featuring a different behavior.

To investigate the energetic properties of the circuit, let us consider the powers exchanged by the resistor, the capacitor and the memristor during the previous experiments. Taking into account equation (22), the powers (in normalized units of measure) of the three elements along the branches mentioned before are given by

$$iv_R = Ri^2 = \frac{RG^2(\varphi_M)}{(1 + RG(\varphi_M))^2} v_C^2 \ ,$$
$$iv_C = -\frac{G(\varphi_M)}{1 + RG(\varphi_M)} v_C^2 \ ,$$
$$iv_M = -iv_C - iv_R = \frac{G(\varphi_M)}{(1 + RG(\varphi_M))^2} v_C^2 \ .$$

Figs. 9A and 9B depict those powers during the evolutions starting, respectively, from A and B. In the first case, all the energy is provided by the capacitor, whose load depends on the initialization. The resistor and the memristor consume that energy until a steady state is reached, so the memristor acts exactly as a resistance. In the second case, instead, the capacitor has almost no energy stored, and the initial dynamics is sustained by the memristor, which provides energy to both the resistor and the capacitor, that stores it for the last part of the trajectory, when the memristor helps the resistor to dissipate it. Since the energetic balance of the capacitor is zero, all the energy is generated by the memristor, and it is dissipated by the resistor and the memristor itself.

Figs. 9C and 9D show the evolution of the powers, while the circuit follows the two different branches of the same first integral starting from C or D. As one can notice, the power profiles of the three elements are the same in both the cases. That is, indeed, expected, because G is even and the two branches are odd. What is important here, it is that two identical energetic behaviors bring the circuit into two different final steady states, starting (close) from the same initial condition. As in the case of Fig. 9B, the initially stored energy is almost zero and so the dynamics is sustained only by the memristor, that at the beginning acts as a power source, while later it switches to a passive behavior.

Finally, consider also the following experiments. Denote as C* the fixed point the circuit converges to when initialized at C. Then, perform two perturbations involving a change of first integral, i.e., assume that the perturbed system is started once from point E= $(-1.732, -0.666)$ and another time from F= $(-1.732, 0.666)$, as depicted in Fig. 8. Then, the state reaches two very different steady states, namely $(2.196, 0)$ and $(-2.196, 0)$, with the energetic diagrams reported in Figs. 9E and 9F, respectively. From the analysis of Section 3.4, in the first case the trajectory is bound to move from the left to right towards higher values of φ_M spanning the interval where, according to (27), the power of the

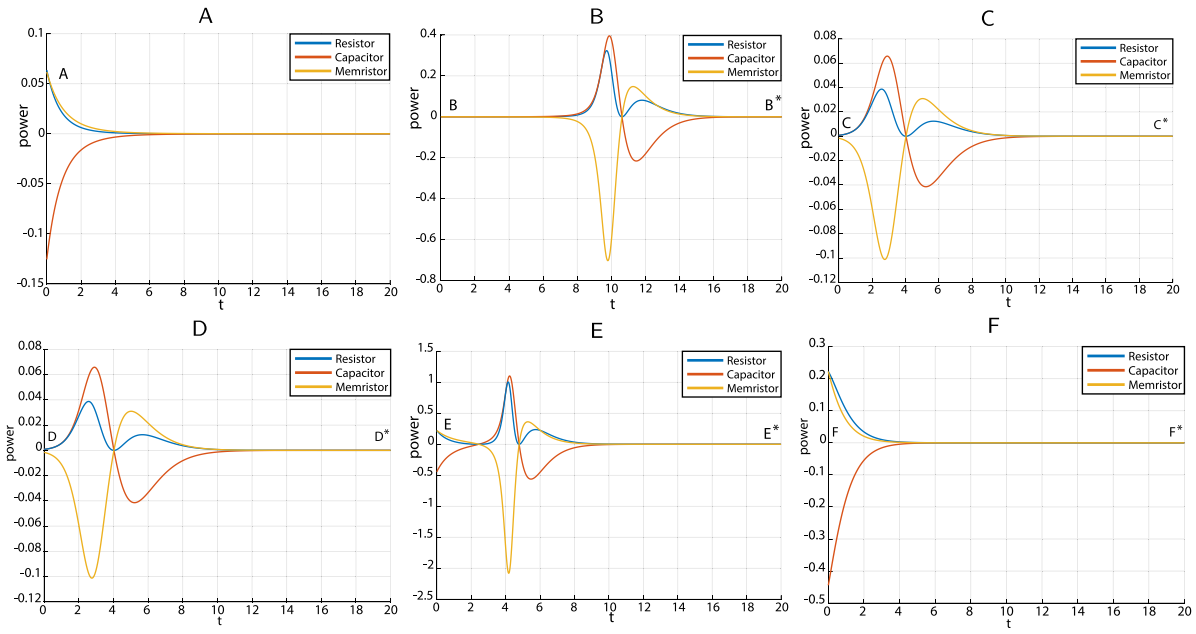

Fig. 9. Energetic behavior of the circuit depicted in Fig. 1, according to the analysis of Section 4. The six scenarios, from A to F, are related to the trajectories with the same label as reported in Fig. 8. Positive values of the power correspond to consumption, while the negative ones to the generation. While the resistor only consume energy, the capacitor and the memristor can perform as both passive and active elements. Notice that "symmetric" trajectories provide equal portraits of the energy. (For interpretation of the references to color in this figure legend, the reader is referred to the web version of this article.)

memristor is negative, i.e., it is generated. In the second case, instead, the locally active region $(-1, 1)$ is never crossed, because the orbit evolves towards lower values of φ_M, and so the memristor acts as a resistor.

The above experiments highlight some important features. As known, depending on its characteristic function (i.e. memristance or memductance) the memristor can be locally active. Notably, the considered circuit always ends in a state associated with no energy left, i.e. the memristor can only provide energy that vanishes as the time passes by, because all the trajectories will eventually land into the fixed points at $v_C = 0$. Nevertheless, this feature is not specific of the memristor itself, but it emerges from the nature of the first integrals for the considered circuit. Indeed, in this state space they are cubic shaped functions divided in branches by the intersection with the axis $v_C = 0$, which consists of an infinite number of non isolated fixed points. By the previous analysis of Section 3.4, it is straightforward to verify that each trajectory finally reaches one of these fixed points, and, therefore, that all the starting energy is somehow dissipated, even if there can be a "local" injection from the memristor. This is particularly clear, when the capacitor augments its energy thanks to the power supplied by the memristor. However, such a scenario is strictly dependent on the circuit, and, in general, more various energetic situations have to be expected, even those where the final regime is powered only by the memristor.

For the sake of completeness, consider the circuit depicted in Fig. 1 and studied in Section 2.1. As illustrated in Figs. 2 and 3, depending on the initialization of the first integral, the circuit dynamics can approach a steady state or a periodic solution. In the second case, since the circuit has a resistor which dissipates energy, some energy is necessary to sustain the periodic regime. The capacitor and the inductor are not able to indefinitely power the circuit because they can store only a finite though arbitrary quantity of energy fixed at the initialization. Therefore, the regime is necessarily sustained by the memristor, thus turning out to be an important device in the design of oscillating and multistable circuits.

The richness of behaviors illustrated so far shows that what actually gives the energetic characterization is not the memristor itself, but rather the dynamics on the first integrals. How the voltage and current of the memristor vary along the first integral is, indeed, what defines its active or passive role, and such a feature depends on the nature of the branch where the orbit evolves. In this respect, it is worth stressing that the first integral is properly referred to the trajectory, and it does not describe a potential energy, as in many Hamiltonian systems. In the same way, it turns out that the "memory" of the memristor does not correspond to a storing property of the energy, but, rather, it emerges from its own state variable, which provides an "integral effect" on the input despite this has no specific energetic implications.

5. First integrals in circuits with generalized memdevices of higher order

In this section we introduce a class of ideal memdevices, which extends the ideal memristors in the direction of increasing the order of their internal dynamics. We call them "ideal," because, as we will show hereafter, they are able to generate first integrals of the motion. As it will be clear later, these devices turn out useful also for addressing the problem of the loss of ideality in a generalized framework.

We denote as *Ideal Generalized Memdevice* an electronic element that is described in proper units of measure by a model of the form:

$$\begin{cases} M_0^{-1}(D)x = y \\ u = N_0^{-1}(D)H(x) \end{cases}, \tag{28}$$

where $H(\cdot)$ is a sufficiently smooth function, and $M_0(\cdot)$ and $N_0(\cdot)$ are polynomial rational functions, which admit the following structure:

$$M_0(D) = \frac{\Phi_M(D)}{D\Psi_M(D)}, \quad N_0(D) = \frac{\Phi_N(D)}{D\Psi_N(D)}. \tag{29}$$

We assume that both $M_0(D)$ and $N_0(D)$ are causal, but possibly not strictly (which makes $M_0^{-1}(D)$ and $N_0^{-1}(D)$ possibly non strictly anti-causal), i.e. $\deg \Phi_M \leq \deg \Psi_M + 1$ and $\deg \Phi_N \leq \deg \Psi_N + 1$. Moreover, we assume that the numerator and the denominator of $M_0(\cdot)$ and $N_0(\cdot)$ are coprime (that implies $\Phi_M(0) \neq 0$ and $\Phi_N(0) \neq 0$), and for the sake of the simplicity we also enforce two technical conditions

$$\Psi_M(0) \neq 0\,, \quad \Psi_N(0) \neq 0\,.$$

Notice that, for proper configurations of the parameters of $M_0(D)$ and $N_0(D)$, model (28) comprises all the ideal memelements along with

mild assumptions on the regularity of their nonlinear characteristic functions. For instance, the ideal memristor emerges from $M_0(D) = D^{-1}$ and $N_0(D) = D^{-1}$, which turn model (28) into

$$\begin{cases} Dx = y \\ u = DH(x) = \dfrac{\partial H(x)}{\partial x} Dx = G(x)y \end{cases} .$$

In this case the regularity assumption boils down to the integrability of the characteristic function $G(\cdot)$. The ideal φ-controlled memcapacitor, instead, comes from choosing $M_0(D) = D^{-1}$ and $N_0(D) = D^{-2}$ (see [34]):

$$\begin{cases} Dx = y \\ \xi = DH(x) = \dfrac{\partial H(x)}{\partial x} Dx = G(x)y \\ u = D\xi \end{cases} .$$

Finally, the ideal ρ-controlled meminductor is obtained from $M_0(D) = D^{-2}$ and $N_0(D) = D^{-1}$ (e.g., see again [34]):

$$\begin{cases} D\xi = y \\ Dx = \xi \\ u = DH(x) = \dfrac{\partial H(x)}{\partial x} Dx = G(x)\xi \end{cases} .$$

Let us now connect the ideal generalized memdevice (28) to the usual circuit Σ. Then, the complete system turns out described by the nonlinear differential equation

$$y = L(D)u = L(D)N_0^{-1}(D)H\left(M_0(D)y\right)$$

that can be more conveniently formulated as

$$y - \frac{P(D)}{Q(D)} N_0^{-1}(D)H\left(M_0(D)y\right) = 0 .$$

Then, transform it applying to both the sides the operator $\Phi_N(D)Q(D)$

$$\Phi_N(D)Q(D)y - D\Psi_N(D)P(D)H\left(M_0(D)y\right) = 0$$

and, finally, integrate with D^{-1}, thus obtaining

$$\Phi_N(D)Q(D)D^{-1}y - \Psi_N(D)P(D)H\left(M_0(D)DD^{-1}y\right) = w_0 ,$$

where w_0 is a constant. If we define

$$z = D^{-1}y ,$$

then the above equation can be rewritten as

$$\Phi_N(D)Q(D)z - \Psi_N(D)P(D)H\left(\Phi_M(D)\Psi_M^{-1}(D)z\right) = w_0 , \tag{30}$$

which is a first integral, as well as a nonlinear non-homogeneous differential equation representing the dynamics of the whole circuit seen from the point of view of z. Therefore, the memdevices of the proposed form (28) are able to induce for the same class of circuit Σ the existence of first integrals of the motion.

To disclose the nature of z further, denote

$$R_0(D) = \frac{\Psi_N(D)}{\Phi_N(D)} , \tag{31}$$

$$S_0(D) = \frac{\Phi_M(D)}{\Psi_M(D)} , \tag{32}$$

$$U(D) = \frac{1}{\Phi_N(D)Q(D)} , \tag{33}$$

so that its dynamics reads

$$z - L(D)\Big(R_0(D)H\big(S_0(D)z\big)\Big) = U(0)w_0 ,$$

which represents a feedback system subject to the external forcing input $U(0)w_0$, where the feed-forward branch can be characterized by the original linear subsystem $L(D)$ representing Σ, and the feedback loop is implemented by the nonlinear dynamic filter $R_0(D)H\big(S_0(D)z\big)$, as depicted in Fig. 10.

Remark 1. As in the case of the ideal memristor, the first integral induced by the proposed ideal memdevice (28) is defined on a variable z, which is the integral of the output y of the memdevice along the state space trajectory.

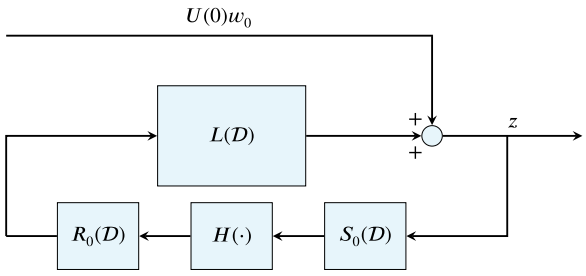

Fig. 10. Schematics of the structure investigated in Section 5.

6. Loss of ideality

The first integral studied in Section 3 is a structural feature of circuits with an ideal memristor, and it can be extended to more general cases as explained in Section 3.1 and Section 5. In this section we investigate what happens when the "ideality" is lost, intending this as the destruction of the layered structure induced by the first integral of the motion. To this aim, we will develop a non-ideal device capable of collapsing onto an ideal generalized memdevice, when two tuning coefficients ε and δ tend to zero. As it will be shown, when the non-ideal circuit is close enough to its ideal counterpart, its behavior retains as an hidden dynamics the ideal behavior, simplifying its analysis.

The loss of ideality mechanism that will be proposed later is motivated by the following examples.

6.1. Motivating example: Leaky integral

Let us consider a memdevice described by the following equations:

$$\begin{cases} (D + \varepsilon)x = y \\ u = G(x)y \end{cases} . \tag{34}$$

When $\varepsilon = 0$, it coincides with an ideal memristor model, and so ε measures how close they are. Model (34) does not describe an ideal memristor anymore, because it implements a defective integral. We assume $\varepsilon > 0$, which implies that x opposes the integration itself, avoiding a pathological unnatural divergence. We refer to such a process as "leaky integral model." As before, function $G(\cdot)$ is assumed integrable with respect to x, i.e. $G(x) = \frac{\partial}{\partial x}H(x)$ for a proper function $H(\cdot)$. Then, observe that this time

$$DH(x) = G(x)Dx = -\varepsilon G(x)x + G(x)y ,$$

which leads first to

$$G(x)y = DH(x) + \varepsilon G(x)x$$

and eventually to

$$u = (D + \varepsilon)H(x) + \varepsilon\big(G(x)x - H(x)\big) .$$

Let us now connect the non-ideal memdevice (34) to the circuit Σ described by $y = L(D)u = (P(D)/Q(D))u$, thus obtaining the overall dynamics

$$y - L(D)(D + \varepsilon)H(x) - \varepsilon L(D)\big(G(x)x - H(x)\big) = 0 .$$

A direct comparison with the ideal memristor case (11) confirms the convergence towards that case when $\varepsilon \to 0$. Then, apply the operator $(D + \varepsilon)^{-1}$ to both the sides, thus obtaining

$$(D + \varepsilon)^{-1}y - L(D)H(x) \quad - \varepsilon L(D)(D + \varepsilon)^{-1}\big(G(x)x - H(x)\big) = v ,$$

where $v(t)$ satisfies

$$(D + \varepsilon)v(t) = 0 \quad \forall t .$$

Notice that v must be a solution of the differential equation

$$Dv = -\varepsilon v \ .$$

For the sake of the notation, denote as Δ the nonlinear operator

$$\Delta(x) = G(x)x - H(x) \ .$$

Then, observing that $(D+\varepsilon)^{-1}y = x$, we have that

$$x - L(D)H(x) - \varepsilon(D+\varepsilon)^{-1}L(D)\Delta(x) = v \ .$$

The above equation can be rewritten in the form

$$x = L(D)\left(H(x) + \xi\right) \ , \tag{35}$$

$$\xi = \frac{\varepsilon}{D+\varepsilon}\eta + v \ , \tag{36}$$

$$\eta = \Delta(x) \ , \tag{37}$$

which is convenient to analyze the structure of the complete system. Notice that x is generated as the output of $L(D)$ by means of two feedback loops. The first one is due to the nonlinear operator H, while the second has a more complex genesis, because according to (36) and (37) it is born from the exogenous input v and a linear filtering (parametric in ε) of η, that is a nonlinear transformation of x itself. It is also worth observing that

$$D\xi = -\varepsilon(\xi - \eta) \ ,$$

where we have exploited that $(D+\varepsilon)v = 0$. Observe that, when all the state variables are bounded, there is a relationship between ε and the dynamics of ξ, because the smaller ε, the slower ξ.

Let us now investigate the relationship between the leaky integral case and the standard formulation (15). To this aim, rewrite (35) as

$$Q(D)x - P(D)H(x) = Q(D)\xi = w \ .$$

Thus, a direct comparison with (15) reveals that the left hand side is just the dynamic structure generating the first integral, while, on the right hand side, the constant input w_0 has been replaced by a more general signal w, which depends on ξ and so on v and x itself.

Remark 2. The dynamics of the first integral is still an important part of the system, which affects its evolution. Nonetheless, since it is not driven by a constant input any more, it may turn out very hard to spot it out from the simple observation of the trajectories. When $\varepsilon \to 0$, ξ converges to a constant value and so does w. Otherwise, the footprint of the first integral emerges only if its relative strength overwhelms that of w.

In order to illustrate the practical meaning of the above remark, hereafter, we consider the same circuit Σ as in the example of Section 3.2, where the memristor has been replaced by the leaky memdevice

$$\begin{cases} Dx = -\varepsilon x + v_M \\ i_M = G(x)v_M \end{cases} .$$

The complete circuit, then, is described by the following system:

$$\begin{cases} Dv_C = -\dfrac{1}{C}\left(\dfrac{1}{R}v_C + i_L + G(x)v_C\right) \\ Di_L = \dfrac{1}{L}v_C \\ Dx = -\varepsilon x + v_C \end{cases} .$$

The numerical simulations, generated using the same configuration as in Section 3.2, are reported in Figs. 11A, 11B, 11C, and 11D for different values of ε, showing how the trajectories tend to act similarly to the ideal case when ε is sufficiently small. In particular, starting from initial conditions placed on different first integrals related to the case $\varepsilon = 0$, the trajectories are drawn onto very slow transients which retain the same shape of the attractors found in the ideal scenario. This property justifies the analysis of the ideal case as a reference framework for non-ideal scenarios.

6.2. Motivating example: Nonlinear reminder

A second different case of loss of ideality is considered, and the corresponding non-ideal memdevice is modeled as follows:

$$\begin{cases} Dx = y \\ u = G(x)y + \delta T(y) \end{cases} , \tag{38}$$

where $T : \mathbb{R} \to \mathbb{R}$ is a generic sufficiently smooth function, and δ is a tuning parameter with the same role previously played by ε in model (34). The main difference with respect to the ideal case is the presence of the term $T(y)$, that can be regarded as a nonlinear static element enhancing the action of an ideal memristor. For instance, if we are talking of a flux-controlled memristor, memdevice (38) can be interpreted as the parallel of an ideal φ-memristor and a nonlinear resistor with admittance δT as in [41]. In the case of a charge-controlled memristor, instead, the memdevice represents the series of q-controlled memristor and a nonlinear resistor with resistance δT.

In general, this additional effect can be seen as the extension to the combination of circuit Σ with a nonlinear device, whose effects are visible from the same port where the memristor is connected to. Roughly speaking, if Σ is nonlinear, but it can be modeled as a linear circuit with a nonlinear element, the "reminder", insisting directly at least on one of the terminals where it is connected to the memristor, then model (38) can be applied.

The interconnection between memdevice (38) and the linear one-port circuit Σ reads, under the usual assumptions,

$$y - L(D)\big(G(x)y + \delta T(y)\big) = y - L(D)DH(x) + \delta L(D)T(Dx) = 0 \ .$$

First, apply on both the sides the operator $Q(D)$

$$Q(D)y - P(D)DH(x) + \delta P(D)T(Dx) = 0$$

and, then, integrate the whole equation applying D^{-1} on both sides

$$Q(D)x - P(D)H(x) + \delta D^{-1}P(D)T(Dx) = w_0 \ , \tag{39}$$

where it has been exploited that $D^{-1}y = x$. Notice that, in general, this equation is not a first integral, because it does not involve only the state coordinates $D^n x, \dots, Dx, x$. Indeed, $P(0) \neq 0$ and the time integral of a nonlinear function $T(Dx)$ is not expected to depend only on the variables x and Dx. Nonetheless, when $\delta \to 0$ equation (39) converges to (15), which is a proper first integral. This latter is still part of the system behavior when $\delta \neq 0$, even if the non constant term $w_0 - \delta D^{-1}P(D)T(Dx)$ can lead it beyond this evidence. Therefore, the loss of ideality does not completely erase the dynamic features once given by the first integrals structure. Nonetheless, as in a slow-fast system, they emerge clear only when δ is sufficiently small.

Finally, observe that (39) can be rewritten as

$$x - L(D)\big(H(x) + \delta D^{-1}T(Dx)\big) = Q(0)w_0 \ ,$$

which, again, describes a forced system with two distinct feedback loops, one featuring the static nonlinear operator H, and another featuring the dynamic nonlinear operator $D^{-1}T(Dx)$.

6.3. Generalized model for the loss of ideality

Based on the illustrative examples of Sections 6.1 and 6.2, we develop a structured model for the loss of ideality based on the ideal generalized memdevice class (28) introduced in Section 5. In our work, the "loss of ideality" is born from breaking a first integrals structure with a driving feedback. In general, many other concepts can be envisioned around the term "ideality," but here we investigate it only for what concerns the existence of the first integrals, since they have been revealed crucial for generating coexistence of attractors.

We propose the following non-ideal memdevice model:

$$\begin{cases} M_\varepsilon^{-1}(D)x = y \\ u = N_\varepsilon^{-1}(D)H(x) + \delta T(y) \end{cases} , \tag{40}$$

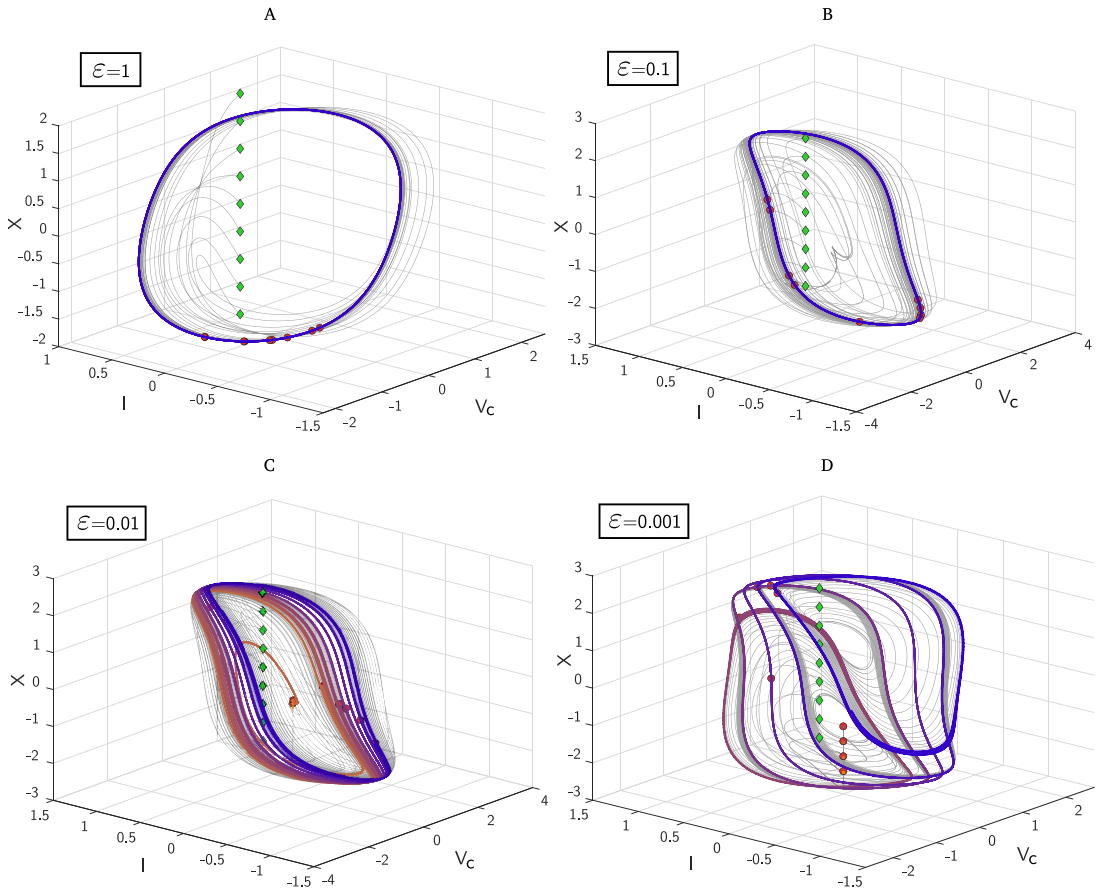

Fig. 11. Starting from the same initial conditions (green diamonds), the trajectories of the circuit illustrated in Section 6.1 are portrayed for different values of the parameter ε. In the cases A and B, after a transient (gray lines), all the orbit reach the same limit cycle. The red circles, laying almost exactly on the circle, denote the final points of the numerical simulations. In the cases C and D, instead, after a transient the trajectories spend a very long time close to structures which resemble limit cycles, but they are not. In fact, a drift that makes those trajectories moving away from those almost cyclic structures is present, but it is as less evident as ε grows smaller. Observe that sometimes in cases C and D the trajectory almost lands on a single point that is a remnant of an equilibrium of the ideal dynamics (that is recovered for $\varepsilon = 0$. (For interpretation of the references to color in this figure legend, the reader is referred to the web version of this article.)

where

$$M_\varepsilon(D) = \frac{\Phi_M(D)}{D\Psi_M(D) + \varepsilon Y_M(D)} ,$$

$$N_\varepsilon(D) = \frac{\Phi_N(D)}{D\Psi_N(D) + \varepsilon Y_N(D)} .$$

We also assume

$$\Phi_M(0) \neq 0 \ , \ \Phi_N(0) \neq 0 \ , \ Y_M(0) \neq 0 \ , \ Y_N(0) \neq 0$$

to avoid cancellations, and

$$\deg \Phi_{M,N} \leq \deg \Psi_{M,N} + 1$$

to guarantee the causality of M_ε and N_ε. For the sake of the simplicity we also enforce the condition

$$\deg Y_{M,N} \leq \deg \Psi_{M,N}$$

to avoid that the degree of the denominators of M_ε and N_ε may change for $\varepsilon = 0$. Notably, when $\varepsilon \to 0$, M_ε and N_ε get the same form of the M_0 and N_0 already seen in (29).

Then, connect the memdevice to the usual circuit Σ, thus obtaining

$$y = L(D)u = L(D)\left(N_\varepsilon^{-1}(D)H(x) + \delta T(y)\right) .$$

The application of the operator $Q(D)\Phi_N(D)$ to both the sides brings to

$$\Phi_N(D)Q(D)y = \left(D\Psi_N(D) + \varepsilon Y_N(D)\right)P(D)H(x) + \delta\Phi_N(D)P(D)T(y) .$$

Rearranging the above equation leads to

$$\Phi_N(D)Q(D)y - D\Psi_N(D)P(D)H(M_\varepsilon(D)y)$$
$$= \varepsilon Y_N(D)P(D)H(M_\varepsilon(D)y) + \delta\Phi_N(D)P(D)T(y) . \quad (41)$$

In general, the terms $D\Psi_N(D)P(D)H(M_\varepsilon(D)y)$, $Y_N(D)P(D)H(M_\varepsilon(D)y)$, and $\Phi_N(D)P(D)T(y)$ are not functions of Dy and other higher order derivatives of y, and, therefore, a first integral cannot be found using the procedure of Section 3. Nonetheless, denote $z = D^{-1}y$ and let us integrate the above Eq. (41):

$$\Phi_N(D)Q(D)z - \Psi_N(D)P(D)H(M_\varepsilon(D)Dz)$$
$$= \varepsilon D^{-1}Y_N(D)P(D)H(M_\varepsilon(D)Dz) + \delta D^{-1}\Phi_N(D)P(D)T(Dz) + w_0 . \quad (42)$$

As noticed, this is not a first integral, but the comparison with (30) highlights that it still retains the same layered structure, even though it is spoiled by additional terms depending on the parameters ε and δ. Anyway, when both $\varepsilon \to 0$ and $\delta \to 0$, the first integral seen in the ideal case (30) lives again. Hence, also in this situation we can interpret the dynamics of the system as trajectories, which move across a structure made of first integrals under the additive effects of a forcing signal.

For the sake of a better understanding, let us introduce the following linear filters

$$U(D) = \frac{1}{\Phi_N(D)Q(D)} ,$$

$$R_\varepsilon(D) = DM_\varepsilon(D) = \frac{D\Phi_M(D)}{D\Psi_M(D) + \varepsilon Y_M(D)} ,$$

$$S_\varepsilon(D) = D^{-1}N_\varepsilon^{-1}(D) = \frac{D\Psi_N(D) + \varepsilon Y_N(D)}{D\Phi_N(D)} ,$$

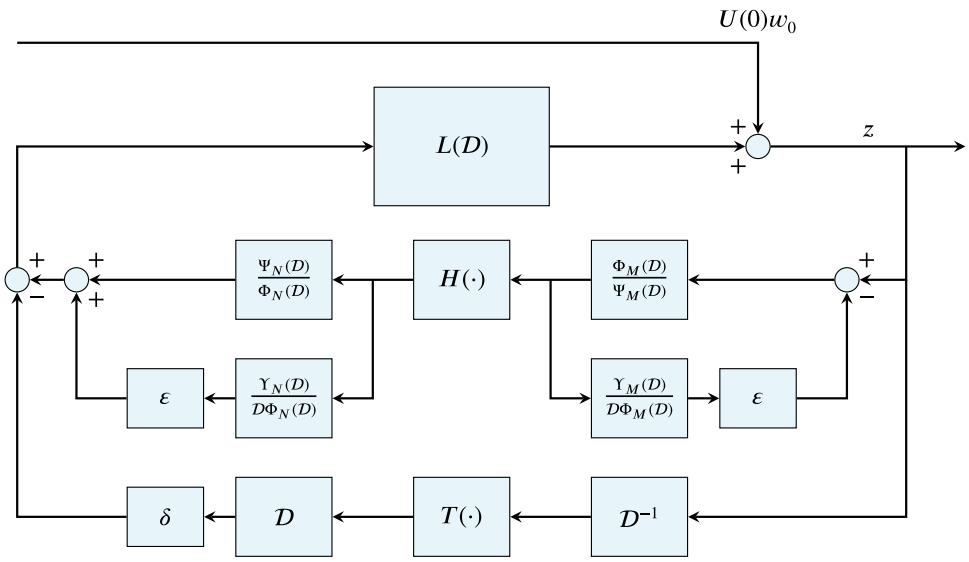

Fig. 12. Schematics of the structure describing the dynamics of system (43), that models a non-ideal generalized memdevice (40) connected to the linear circuit Σ introduced in Section 3.

so that (42) can be rewritten in the form

$$z - L(D)\Big(S_\varepsilon(D)H\big(R_\varepsilon(D)z\big) - \delta D^{-1}T\big(Dz\big)\Big) = U(0)w_0\ . \tag{43}$$

Notice that, when $\varepsilon \to 0$, R_ε and S_ε collapse into the R_0 and S_0 seen in Eqs. (31) and (32). The above equation (43) highlights that the dynamics exhibited by the integral of the motion seen from the perspective of y has the form of a forced feedback system. The driving input is $U(0)w_0$, which depends on the initial conditions of the circuits, while the feedback counts two distinct loops weighted by the parameters ε and δ. The nature of such feedback loops is complex. Indeed, they are the series of a linear filter ($R_\varepsilon(D)$ or $\mathcal{D}$), a nonlinear static operator ($H(\cdot)$ or $T(\cdot)$), and another linear filter ($S_\varepsilon(D)$ or δD^{-1}). See Fig. 12 for a block diagram description.

6.4. Final remarks

Model (40) is capable to induce first integrals in the dynamics of the circuit Σ it is connected to, when $\varepsilon = 0$ and $\delta = 0$. Such a layered structure is lost as soon as at least one of these two parameters is different from zero. Nevertheless, the spoils of the previous first integrals still affect the trajectories, and their influence is as stronger as the parameters are close to zero.

An interesting situation happens when the dynamics of the feedback loops in (43) is particularly slow with respect to the variable z. Such a condition is equivalent to say that the terms $\varepsilon D^{-1}Y_N(D)P(D)H(M_\varepsilon(D)\mathcal{D}z)$ and $\delta D^{-1}\Phi_N(D)P(D)T(Dz)$ in (43) provide small contributions, which can be regarded as negligible perturbations of w_0. Hence, the system behaves close to the first integral dynamics, which comes back in evidence. For instance, if the contribution from the feedback loops dynamics has the form of a monotone drift, then, the visible effect is to slowly change the dynamics from an apparent first integral to another, so much that in a short time frame the observed behavior is indistinguishable from that of a fixed first integral, similarly to what happens in the circuit of Fig. 11.

Model (40) extends the class of the ideal generalized memdevices (28), providing an articulate but smooth mechanism to spoil their first integrals structure, and it is a candidate for describing real memristive devices.

7. Conclusions

In this paper we have investigated the ability of ideal memristors to generate first integrals of the dynamics, when connected to a broad class of circuits featuring linear elements. Extensions to the multiple memristors case, to other ideal memelements, and to the presence of voltage and current sources as well as nonlinear electronic elements can be readily derived using the same approach. The main property connected to the first integrals is that the whole dynamics of the circuit can be described by a reduced order model parameterized by the initial configuration, which acts as a forcing input. This simplifies the analysis, but overall it reveals that the first integrals set up a layered structure of invariant manifolds in the state space of the circuit, where each leaf is induced by the choice of the circuit initial conditions. This feature turns out to be a powerful tool to investigate the system dynamics, and it can be fruitfully exploited to disclose the nature of the so called "extreme multistability," i.e. the incredible number of coexisting attractors, which can populate the state space of a circuit with ideal memristors. Notably, the initial conditions, which determine the appearance of each attractor, structurally act as an external input driving a nonlinear feedback system. Reasoning on this interpretation, we have designed a new class of ideal devices, which are capable of inducing the same first integrals structure, and on this premise we have developed a mechanism for the loss of the ideality, whose task is to spoil the layered state space. Notably, even when the first integrals are no longer present, their legacy still affects the circuit dynamics, even if it may be hard to spot their evidence. It is believed that the generality of the introduced non-ideal memdevices may help in modeling real implementations of memristive elements.

CRediT authorship contribution statement

Giacomo Innocenti: Writing – review & editing, Writing – original draft, Visualization, Software, Methodology, Investigation, Formal analysis, Conceptualization. **Alberto Tesi:** Writing – review & editing, Methodology, Conceptualization. **Mauro Di Marco:** Writing – review & editing, Methodology, Conceptualization. **Mauro Forti:** Writing – review & editing, Methodology, Conceptualization.

Declaration of competing interest

The authors declare that they have no known competing financial interests or personal relationships that could have appeared to influence the work reported in this paper.

Data availability

Data will be made available on request.

Acknowledgments

This work has been supported by the project "Analogue COmputing with Dynamic Switching Memristor Oscillators: Theory, Devices and Applications (COSMO)", Grant PRIN 2017LSCR4K 002, funded by the Italian Ministry of Education, University and Research (MIUR).

References

[1] Chua L. Memristor – the missing circuit element. IEEE Trans Circ Theory 1971;18(5):507–19.
[2] Strukov DB, Snider GS, Stewart DR, Williams RS. The missing memristor found. Nature 2008;453(7191):80–3.
[3] Li Y, Wang Z, Midya R, Xia Q, Yang JJ. Review of memristor devices in neuromorphic computing: materials sciences and device challenges. J Phys D: Appl Phys 2018;51(50):503002.
[4] Zhang Y, Wang Z, Zhu J, Yang Y, Rao M, Song W, et al. Brain-inspired computing with memristors: Challenges in devices, circuits, and systems. Appl Phys Rev 2020;7(1).
[5] Kim SJ, Kim S, Jang HW. Competing memristors for brain-inspired computing. Iscience 2021;24(1).
[6] Venkatesan T, Williams S. Brain inspired electronics. Appl Phys Rev 2022;9(1).
[7] Kumar S, Wang X, Strachan JP, Yang Y, Lu WD. Dynamical memristors for higher-complexity neuromorphic computing. Nat Rev Mater 2022;7(7):575–91.
[8] Mohanty SP. Memristor: from basics to deployment. IEEE Potentials 2013;32(3):34–9.
[9] Mazady A, Anwar M. Memristor: Part I – the underlying physics and conduction mechanism. IEEE Trans Electr Devices 2014;61(4):1054–61.
[10] Wang L, Yang C, Wen J, Gai S, Peng Y. Overview of emerging memristor families from resistive memristor to spintronic memristor. J Mater Sci, Mater Electron 2015;26:4618–28.
[11] Mohammad B, Jaoude MA, Kumar V, Al Homouz DM, Nahla HA, Al-Qutayri M, et al. State of the art of metal oxide memristor devices. Nanotechnol Rev 2016;5(3):311–29.
[12] Vaidyanathan S, Volos C. Advances in memristors, memristive devices and systems, vol. 701. Springer; 2017.
[13] Ascoli A, Slesazeck S, Mähne H, Tetzlaff R, Mikolajick T. Nonlinear dynamics of a locally-active memristor. IEEE Trans Circuits Syst I Regul Pap 2015;62(4):1165–74.
[14] Jin P, Wang G, Iu HH-C, Fernando T. A locally active memristor and its application in a chaotic circuit. IEEE Trans Circuits Syst II 2017;65(2):246–50.
[15] Corinto F, Forti M. Memristor circuits: Flux – charge analysis method. IEEE Trans Circuits Syst I Regul Pap 2016;63(11):1997–2009.
[16] Corinto F, Forti M. Memristor circuits: Bifurcations without parameters. IEEE Trans Circuits Syst I Regul Pap 2017;64(6):1540–51.
[17] Innocenti G, Di Marco M, Forti M, Tesi A. Prediction of period doubling bifurcations in harmonically forced memristor circuits. Nonlinear Dynam 2019;96:1169–90.
[18] Di Marco M, Forti M, Pancioni L, Innocenti G, Tesi A. New method to analyze the invariant manifolds of memristor circuits. J Franklin Inst B 2022;359(18):11007–38.
[19] Di Marco M, Innocenti G, Tesi A, Forti M. Dynamic analysis of memristor circuits via input–output techniques. In: Memristor computing systems. Springer; 2022, p. 21–52.
[20] Kim H, Sah MP, Yang C, Cho S, Chua LO. Memristor emulator for memristor circuit applications. IEEE Trans Circuits Syst I Regul Pap 2012;59(10):2422–31.
[21] Yang C, Choi H, Park S, Sah MP, Kim H, Chua LO. A memristor emulator as a replacement of a real memristor. Semicond Sci Technol 2014;30(1):015007.
[22] Bao B-C, Xu Q, Bao H, Chen M. Extreme multistability in a memristive circuit. Electron Lett 2016;52(12):1008–10.
[23] Bao B, Jiang T, Xu Q, Chen M, Wu H, Hu Y. Coexisting infinitely many attractors in active band-pass filter-based memristive circuit. Nonlinear Dynam 2016;86:1711–23.
[24] Bao B, Wang N, Xu Q, Wu H, Hu Y. A simple third-order memristive band pass filter chaotic circuit. IEEE Trans Circuits Syst II 2016;64(8):977–81.
[25] Di Marco M, Forti M, Corinto F, Chua L. Unfolding nonlinear dynamics in analogue systems with mem-elements. IEEE Trans Circuits Syst I Regul Pap 2020;68(1):14–24.
[26] Dou G, Yang H, Gao Z, Li P, Dou M, Yang W, et al. Coexisting multi-dynamics of a physical SBT memristor-based chaotic circuit. Int J Bifurcation Chaos 2020;30(11):2030043.
[27] Escudero M, Spiga S, Di Marco M, Forti M, Innocenti G, Tesi A, et al. Physical implementation of a tunable memristor-based chua's circuit. In: ESSCIRC 2022-IEEE 48th European solid state circuits conference. IEEE; 2022, p. 117–20.
[28] Di Marco M, Forti M, Pancioni L, Innocenti G, Tesi A, Corinto F. Oscillatory circuits with a real non-volatile stanford memristor model. IEEE Access 2022;10:13650–62.
[29] Peng Y, Sun K, He S. A discrete memristor model and its application in Hénon map. Chaos Solitons Fractals 2020;137:109873.
[30] Bao H, Hua Z, Li H, Chen M, Bao B. Discrete memristor hyperchaotic maps. IEEE Trans Circuits Syst I Regul Pap 2021;68(11):4534–44.
[31] He S, Zhan D, Wang H, Sun K, Peng Y. Discrete memristor and discrete memristive systems. Entropy 2022;24(6):786.
[32] Riaza R. Manifolds of equilibria and bifurcations without parameters in memristive circuits. SIAM J Appl Math 2012;72(3):877–96.
[33] Corinto F, Forti M. Memristor circuits: Pulse programming via invariant manifolds. IEEE Trans Circuits Syst I Regul Pap 2017;65(4):1327–39.
[34] Innocenti G, Di Marco M, Tesi A, Forti M. Input–output characterization of the dynamical properties of circuits with a memelement. Int J Bifurcation Chaos 2020;30(07):2050110.
[35] Di Marco M, Innocenti G, Tesi A, Forti M. Circuits with a mem-element: invariant manifolds control via pulse programmed sources. Nonlinear Dynam 2021;106:2577–606.
[36] Arnold VI. Ordinary differential equations. Springer Science & Business Media; 1992.
[37] Di Marco M, Forti M, Innocenti G, Tesi A. Harmonic balance method to analyze bifurcations in memristor oscillatory circuits. Int J Circuit Theory Appl 2018;46(1):66–83.
[38] Di Ventra M, Pershin YV, Chua LO. Circuit elements with memory: memristors, memcapacitors, and meminductors. Proc IEEE 2009;97(10):1717–24.
[39] Guckenheimer J, Holmes P. Nonlinear oscillations, dynamical systems, and bifurcations of vector fields, vol. 42. Springer Science & Business Media; 2013.
[40] Itoh M, Chua LO. Memristor hamiltonian circuits. Int J Bifurcation Chaos 2011;21(09):2395–425.
[41] Corinto F, Gilli M, Forti M. Flux-charge description of circuits with non-volatile switching memristor devices. IEEE Trans Circuits Syst II 2018;65(5):642–6.